Grid-Forming Converter Angular Speed Freezing to Enhance Transient Stability in 100% Grid-Forming and Mixed Power Systems

Xianxian Zhao, Damian Flynn

School of Electrical and Electronic Engineering, University College Dublin, Dublin 4, D04 V1W8 Republic of Ireland (Tel: +35317161959; e-mail: xianxian.zhao@ucd.ie)

Abstract: The transient stability of a power system depends on the relative divergence of angular speeds between voltage sources during a fault disturbance. A unified angular speed control strategy is proposed here for grid-forming and synchronous machine voltage sources. Specifically, for a system consisting only of grid-forming converters (GFs), the virtual angular speed of all GFs is proposed to be frozen to the pre-fault value, while for a system with a mix of grid-forming converters and synchronous machines (SMs), the virtual angular speed of the GFs should be frozen to the weighted mean of the SM rotor speeds. The proposed freezing techniques are designed to be effective for short-circuit faults, and to be indifferent to phase-jump events. Simulation studies are performed on 100% GF and mixed GF/SM systems for both 3-phase fault and phase-jump events, for a range of GF control settings and system conditions, to demonstrate the effectiveness of the virtual angular speed freezing techniques.

Keywords: Grid-forming converters, synchronous generators, transient stability, virtual angular speed, synchronization stability, short-circuit faults, phase-jump disturbances.

1. INTRODUCTION

As part of efforts to reduce carbon emissions and combat climate change, many power systems are rapidly transitioning towards converter-based variable renewable generation, mainly from wind and photovoltaic sources (Hodge et al., 2020). Existing power converters are mostly controlled as "grid-following", using a phase-locked loop (PLL) to synchronize the voltage angle at the point of common coupling, while injecting power to the grid (Zhao et al., 2021b). As grid-following converters (GLs) rely on following a voltage reference, a point is reached, as their share increases, when they can no longer remain synchronized, even for small disturbances, and thus they are unable to maintain controlled and stable outputs (Zhao et al., 2021b).

Controlling some power converters in a "grid-forming" mode represents one way to tackle these challenges and maintain power system stability, while considering increased use of battery storage (Zhao et al., 2021a). The key difference with grid-following converters is that grid-forming converters (GFs) create their own internal voltage angle. Thus, they offer blackstart capability, and can provide a voltage reference for GL converters. Inherently, GFs can also provide an inertial response, similar to synchronous machines, such that they can maintain their voltage angle and provide an immediate respond to voltage and frequency disturbances. Consequently, grid-forming converters are often seen as a replacement for synchronous machines in future power grids.

Transient stability is defined in Kundur (1994) as the ability to maintain synchronism when subject to severe transient disturbances, such as faults on transmission facilities, loss of generation or a large load. Compared with synchronous machines, GFs can provide much faster and more flexible controllability, but with much lower overcurrent capability (typically 20% of rated current, versus up to seven times for synchronous machines (Denis et al., 2018)) and more diverse control designs. It follows that economically maintaining power system transient stability needs to be carefully studied.

GF transient stability analysis under large faults has been studied, using, for example, phase portrait (Pan et al., 2019), power-angle relationship (Huang et al., 2017, Qoria et al., 2019, Rokrok et al., 2021), and Lyapunov's direct method (Shuai et al., 2018). Many control strategies which involve slowing down changes in GF angular speed have been proposed to enhance GF transient stability under large faults, through reducing the active power reference (Qoria et al., 2019, Shuai et al., 2018), modifying the frequency setpoint (Huang et al., 2017), increasing its inertial constant (Qoria et al., 2020), transiently increasing its damping (Xiong et al., 2021), adopting nonlinear sliding mode control (Eskandari and Savkin, 2020), or directly freezing its angular speed to a pre-fault value (Zhao and Flynn, 2020). In Rokrok (2021), the current reference angle is shown to impact the transient stability of a GF with current reference saturation, with implications for the details of the current limiting strategy. In Choopani (2019), in order to mitigate oscillations between multiple virtual synchronous generators (VSGs) (a type of GF) in a 100% VSG-based system, their active power references are modified based on PID control of the VSG frequency relative to the centre of inertia grid frequency.

Although the effectiveness of the above control strategies has been demonstrated, it is often assumed that the GFs are connected to an infinite bus, such that the system frequency does not change during a fault, and/or that all GFs assume the

same control parameters. In Cheng et al (2020), it is shown that a microgrid containing synchronous generators and VSGs is more prone to transient angle instability under faults than a microgrid containing only VSGs, due to the differences between their speed governors. However, a GF-only grid is not necessarily more stable than a mixed grid if the GFs employ diverse parameter settings and different control strategies, considering the real-world challenges of achieving the same parameters and control strategies for many voltage sources across an entire power system. The main contributions of this paper are summarized as follows:

- Transient stability of 100% GF, and a mix of GF and SM, grids are studied under various fault conditions, assuming diverse parameter settings for the GF/SM voltage sources.
- A unified angular speed control strategy is proposed to enhance transient stability for short circuit faults, i.e. for a system with 100% grid-forming converters, the virtual angular speed of all GFs are proposed to be frozen to their pre-fault value, while for a system involving a mix of GFs and synchronous machines, the GF virtual angular speeds are frozen to the weighted mean of the SM rotor speeds.
- The proposed freezing techniques for short-circuit faults are shown not to impact GF performance under phase-jump events.

The paper is organized as follows: modeling of grid-forming converters and synchronous machines, and the proposed signal freezing techniques are described in Section 2; simulation results and analysis are then presented in Section 3; finally, Section 4 presents the conclusions of the paper.

2. TRANSIENT STABILITY ENHANCEMENT

As part of analyzing and controlling interactions between different voltage sources, individual models of GFs and SMs are first described, before introducing the proposed virtual angular speed freezing techniques for GFs to enhance system transient stability for severe faults.

2.1 Droop control-based grid-forming converter model

Figure 1 shows a voltage source converter (VSC), connecting to the grid through a LCL filter, with a capacitor and PI-controlled DC current source (representing DC bus dynamics and DC input power, such as from a wind turbine, PV or energy storage system). The series impedance (R_c, L_c) is modelled as a transformer. The droop-based control structure and parameters are also shown in Fig. 1. The control includes outer P/f and Q/V droop control loops, and cascaded inner voltage and current PI control loops. Damping enhancement control (Δe_d, Δe_q) and threshold virtual impedance (VI) current limitation control (ΔV_{VId}, ΔV_{VIq}) are also added to the outer loop voltage references, v_{od}^* and v_{oq}^*. To strictly limit the converter current, and compensate for the response time of the VI control, a "hard" current limiter is applied to the d- and q-axis current references, i_{cd}^* and i_{cq}^*. Scaling-down current limitation and anti-windup integration of the voltage PI controller are implemented, as detailed in Zhao and Flynn (2020). Note that the form of the current limitation control greatly affects GF transient stability. Here, VI control (structure and parameters follow Qoria et al. (2018) is used as the main approach to limit the converter current, as it offers better transient dynamics compared to only using a "hard" current saturation approach (Qoria et al., 2019).

2.2 Synchronous machine model

The considered synchronous machine model incorporates an exciter, power system stabilizer (PSS), governor, and prime mover. Frequency loop parameters are from Lin et al. (2017) while the remainder follow Kundur (1994). The SM rotor equation is expressed as

$$2H\dot{\omega}_r = P_m^* - P_e - D(\omega_r - \omega), \qquad (1)$$

where H and D are inertial and damping constants.

To provide a theoretical foundation for the parameter settings of the Section 3 case studies, according to Fig. 1, the P/f

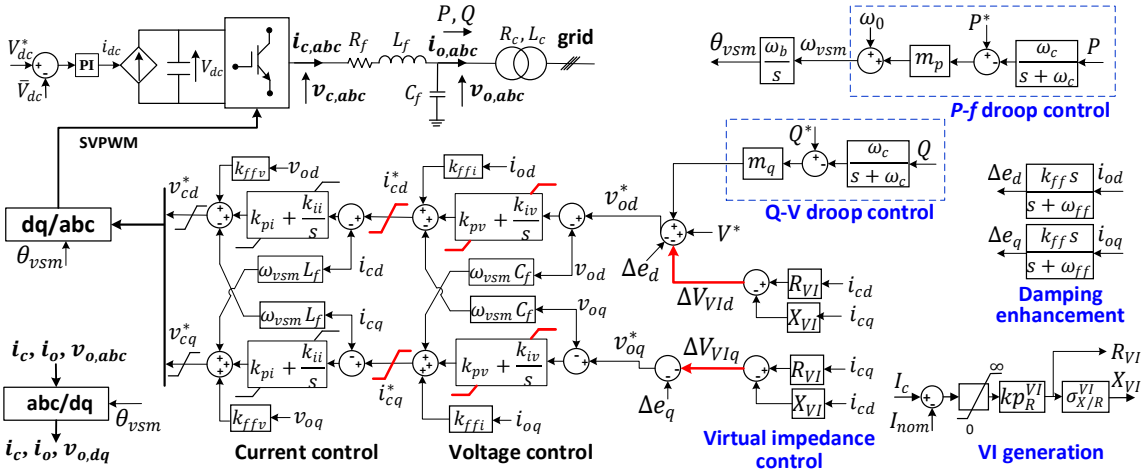

Parameter	Value (pu)	Parameter	Value (pu)
R_f, L_f, C_f,R_c, L_c	0.005, 0.15, 0.066, 0.005, 0.15	k_{pv}, k_{iv}, k_{pi}, k_{ii}	0.52, 1.161022, 0.7388, 1.19
m_p, m_q, ω_0	0.02, 0.0001, 1	$i_{cd}^{*2} + i_{cq}^{*2}$	$\leq 1.25^2$
K_{ffi}, K_{ffv}, ω_{ff}, K_{ff}	1, 1, 16.66, 0.01	K_{VI}, $K_{X/R}$, I_{nom}	0.67, 5, 1
C_{dc}, V_{dc}^*	2 mF, 1	K_p^{dc}, K_i^{dc}	82, 2048

Figure 1. Droop control-based GF connected to a DC current source and a grid via LCL filter, and its control structure and parameters.

droop control loop can be expressed in per-unit as follows

$$\frac{1}{\omega_c m_p}\dot{\omega}_{vsm} = P^* - p_{mes} - \frac{1}{m_p}(\omega_{vsm} - \omega). \qquad (2)$$

Comparing (1) with (2), the equivalent inertia and damping constants for the GF droop-control GF are

$$H_{GF}^{eq} = \frac{1}{2\omega_c m_p}, \qquad D_{GF}^{eq} = \frac{1}{m_p}. \qquad (3)$$

2.3 Transient stability enhancement for a system with 100% grid-forming converters as voltage sources

Grid-forming transient stability is affected by the transient evolution of the voltage angle, and the d- and q-axis components of the generated voltage. Focus here is placed on the former aspects to enhance system transient stability. In practice, a power system may consist of many types of GF, and even those of the same type may employ different parameter settings. Instead of controlling the virtual angular speed or the associated angle for each GF, the virtual angular speed of all GFs is proposed to be frozen to pre-fault values when a fault is detected (see Fig. 2). Hence, the relative angular differences between the GFs when a fault is cleared should be relatively similar to the pre-fault values (variations will occur due to the specific control settings and system conditions). Based on the power-angle relationship and equal area criterion, if the relative angle between voltage sources does not drift too far apart during a fault, the power system is less prone to going unstable during a fault. Moreover, as all GFs are frozen to the same angular speed, the fault critical clearing time should be increased. Finally, as seen in Fig. 2, no communication is required. The frozen angular speed input can be updated, as appropriate, as system conditions change, using (slow) communications, or otherwise.

As shown in Fig. 2, the freezing action is activated when both the output voltage and active power (V and P) are lower than V_l and P_l. Including the P signal helps to prevent the freezing action being activated during grid phase-jump down events. The hysteresis comparators help to avoid frequent switching.

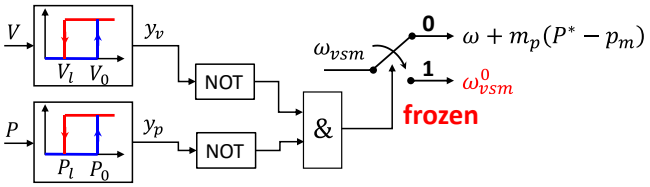

Figure 2. Proposed unified virtual angular speed freezing technique to enhance the transient stability of a 100% GF system, where V_0 and P_0 are the pre-fault output voltage and active power, and V_l and P_l are lower limits (set here as $V_0 - 0.25$ pu and $P_0 - 0.2$ pu).

2.4 Transient stability enhancement for a system with a mix of grid-forming converters and synchronous machines

For a power system with both GFs and SMs, the above unified virtual angular speed freezing technique for GFs is not applicable, since the rotor speed of the SMs cannot be arbitrarily frozen. Therefore, it is proposed that the virtual angular speed of all GFs is frozen to the weighted mean angular speed of all SMs for such a system (see Fig. 3). The weighted mean angular speed of the SMs is calculated as

$$\bar{\omega}_r = \frac{\sum_{i=1}^{N} S_{sgi} H_{sgi} \omega_{ri}}{\sum_{i=1}^{N} S_{sgi} H_{sgi}} \qquad (4)$$

where, S_{sgi}, H_{sgi} and ω_{ri} are the rated capacity, inertial constant, and rotor speed of the i^{th} SM, and N is the total number of SMs. S_{sgi} in (4) accounts for the fault current injection from a SM, while $H_{sgi}\omega_{ri}$ reflects the angle evolution (deduced from (2)). From Fig. 3, communication is required to obtain $\bar{\omega}_r$. Note that only SMs which dominate the response (i.e. large $S_{sgi}H_{sgi}$) are needed to calculate $\bar{\omega}_r$. Moreover, (4) can be calculated for local areas, since voltage sources distant from the fault will have limited impact.

The freezing action is activated when the output voltage and active power (V and P) are lower than V_l and P_l, and rotor speed difference $|\omega_{vsm} - \bar{\omega}_r| \geq \varepsilon_h$. The freezing action is deactivated when $|\omega_{vsm} - \bar{\omega}_r| < \varepsilon_l$. Note that the proposed virtual angular speed freezing techniques in Fig. 2 and 3 can also be applied to other types of GFs.

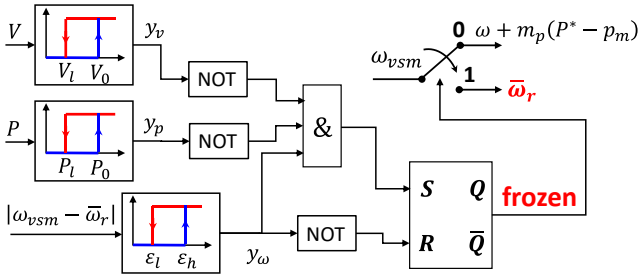

Figure 3. Proposed virtual angular speed freezing technique of GFs to enhance the transient stability of a mixed GF/SM system, where ε_l and ε_h are small positive constants (set here as 0.0004 pu and 0.002 pu), with the remaining parameters unchanged from Fig. 2.

3. CASE STUDIES

Using two simple, illustrative systems (Figs. 4 and 8), 500 ms 3-phase faults are applied in all cases, to support the following observations

(a) Diverging angular speeds between voltage sources during a fault make a system less transiently stable, for both 100% GF and mixed GF/SM systems
(b) The proposed virtual angular speed freezing techniques for GFs (Fig. 2 & 3), can greatly enhance the transient stability of a 100% GF, or mixed GF/SM, system
(c) The proposed virtual angular speed freezing techniques for GFs do not affect performance for phase-jump events

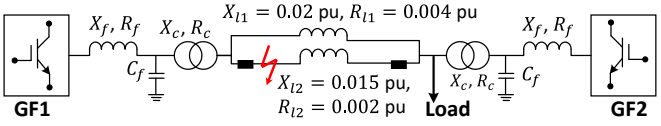

Figure 4. Test system with 100% GFs for Cases 1 – 5, where $R_{l1,2}$ and $X_{l1,2}$ pu values assume a 100 MVA capacity base (The fault is cleared by line disconnection).

3.1 Transient stability assessment of a 100% GF system

Based on the system in Fig. 4, according to (2), Cases 1 – 5 are defined (Table 1), to investigate how diverging GF angular speeds during a fault make a 100% GF system less stable, compared with all GFs using the same parameter

settings. Case 1 represents the base case, for which both GFs apply the same settings, while Cases 2 – 5 investigate the transient stability impacts of using different GF active power reference, inertia, damping, and capacity & transmission line R/X ratio settings. In Case 5, two changes from Case 1 are introduced, to further lower the system's stability boundary.

The simulation results for Cases 1 – 5 are shown in Fig. 5, which indicate that only under Case 1 is the system stable. The angular speed difference between GF1 and GF2 is the smallest during the fault in Case 1, which demonstrates that

(a) differences in GF parameter settings lead to diverging internal voltage virtual angular speeds during a fault; and
(b) the larger the difference in internal voltage angular speed between GFs the less stable the system will be.

Table 1. Simulation settings for Cases 1 – 5 (S_b in MVA)

	P^* (pu) (GF1/GF2)	ω_c (pu) (GF1/GF2)	m_p (pu) (GF1/GF2)	S_b & R_{l1}, R_{l2} & L_{l2} (pu)
Case 1	0.9	31.4	0.02	500 & 0.004
Case 2	**0.9/0.3**	31.4	0.02	500 & 0.004
Case 3	0.9	**125.6/1.5**	0.02	500 & 0.004
Case 4	0.9	31.4	**0.02/0.001**	500 & 0.004
Case 5	0.9	31.4	0.02	**50/950 & 0.04, 0.1 & 0**

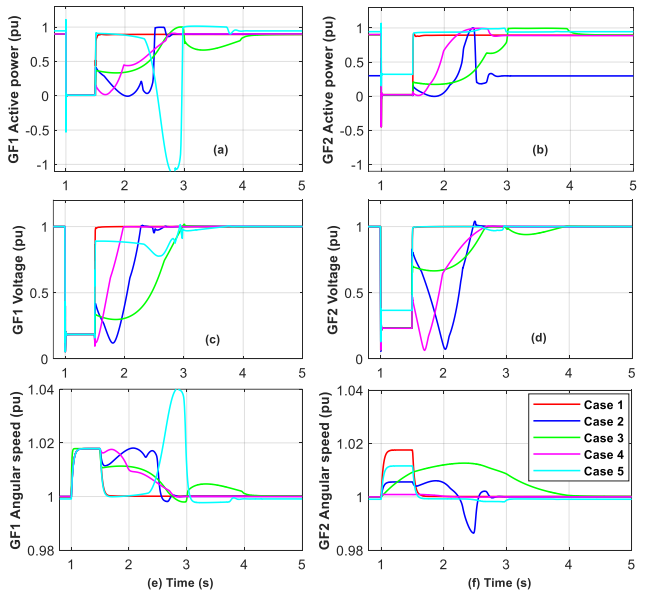

Figure 5. Cases 1 – 5 for different GF1 and GF2 settings, which lead to different angular speeds during the 500 ms, 3-phase fault.

3.2 GF virtual angular speed freezing to pre-fault value technique for a 100% GF system

Cases 1 – 5 are now reconsidered with both GFs applying the virtual angular speed freezing technique proposed in Fig. 2. With the virtual angular speeds of GF1 and GF2 being frozen to their pre-fault values (see Fig. 6(e)(f)), the previously unstable Cases 2 – 5 (Fig. 5) are now stabilized. Meanwhile, Case 1 exhibits very similar dynamics, with, and without, the proposed freezing technique, demonstrating its effectiveness for enhancing the transient stability of a 100% GF system.

Based on Case 2, Cases 6 – 8 are now simulated (see Table 2), where the virtual angular speeds of both GFs are now frozen to ω_{vsm}^0, $\omega_{vsm}^0 + 0.1$, and $\omega_{vsm}^0 - 0.1$ pu, respectively. Fig. 7(a)(b) show that the active power outputs of both GFs are coincident, while Fig. 7(c)(d) show similar voltage profiles, during and post-fault, despite the differences in the setting for the three frozen angular speeds. Fig. 7(c)(d) also show that during the fault, the GF voltages are highest under Case 7 and lowest under Case 8, which demonstrates that

(a) unified freezing of GF virtual angular speed during a fault can enhance the transient stability of a 100% GF system, with the choice of frozen value not critical;
(b) freezing the GF virtual angular speed to a value above the pre-fault level can better support the local voltage.

Table 2. Simulation settings for Cases 6 – 8

	Case 6	Case 7	Case 8
ω_{vsm} frozen during a fault (pu)	$\boldsymbol{\omega_{vsm}^0}$	$\boldsymbol{\omega_{vsm}^0 + 0.1}$	$\boldsymbol{\omega_{vsm}^0 - 0.1}$

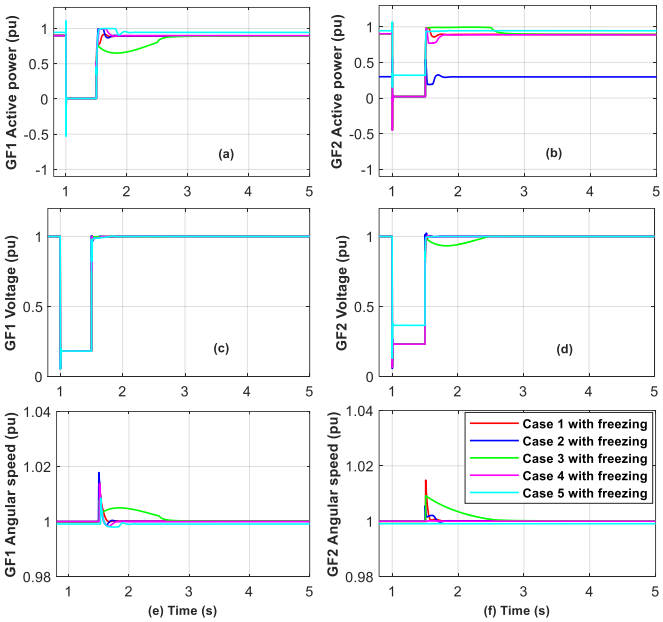

Figure 6. Cases 1 – 5 with both GFs incorporating virtual angular speed freezing, for a 500 ms, 3-phase fault.

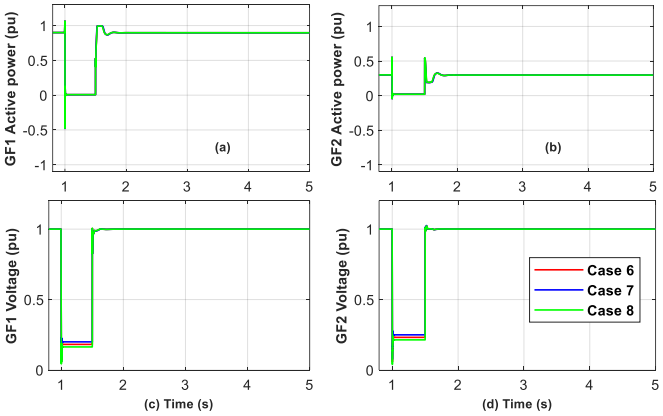

Figure 7. Cases 6 – 8, based on Case 2, incorporating virtual angular speed freezing, with GF angular speed frozen to ω_{vsm}^0, $\omega_{vsm}^0 + 0.1$ and $\omega_{vsm}^0 - 0.1$ pu.

3.3 Transient stability assessment of a mixed GF/SM system

The mixed GF/SM system of Fig. 8 is simulated under Cases 9 – 11, using the Table 3 settings. Fig. 9(a)-(d) show that the system is stable in Case 9 with H_{sg} high (6 s), but unstable in Case 10 with H_{sg} low (2 s). As seen from Fig. 9(e)(f), the underlying problem is that the angular speed difference between the GF and SG is smaller in Case 9 than in Case 10. Case 11 reduces the GF equivalent inertia, towards zero, by increasing ω_c, which reduce the angular speed difference (of Case 10) and stabilizes the system, if slowly (≈1.5 s after fault clearance). Further reducing H_{sg} in Case 11 causes the system to become unstable (not shown here). Instead, in order to reduce the angular speed difference between the GF and SG (to enhance transient stability), m_p should be increased, which reduces D_{GF}^{eq}, based on (3). However, GF stability restrictions imply that m_p must be small (Qoria et al., 2018). It follows that GFs have some, but limited, ability to enhance the transient stability of a mixed GF/SM system, by adjusting control parameters alone.

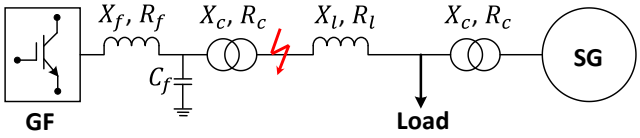

Figure 8. Test system for Cases 9 – 13, where the default GF and SG capacities and power references are unchanged from Case 1, with differences marked in red in Tables 3 and 4.

Table 3. Simulation settings for Case 9 – 11

	Case 9	Case 10	Case 11
H_{SG}	**6 s**	**2 s**	**2 s**
H_{GF}^{eq}	0.8 s	0.8 s	**0.001 s**

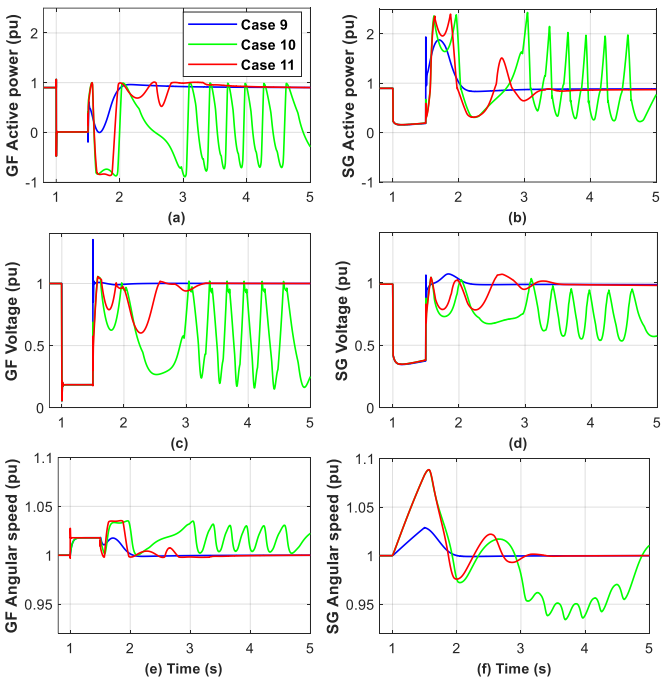

Figure 9. Cases 9 – 11 for different GF and SG inertia values.

3.4 GF virtual angular speed freezing to weighted mean rotor speed of SMs technique for a mixed GF/SM system

The mixed system of Fig. 8 is now studied under Cases 12 – 13, with the proposed freezing technique of Fig. 3 applied to the GF, and the SG inertia assumed to be very low (0.5 s). Simulation settings are summarized in Table 4. Comparing Fig. 9 with Fig. 10, Case 12 stabilizes the unstable Case 10. Fig. 10(a)-(d) show that the active power and voltage recover to pre-fault levels ≈0.5 s after fault clearance, even with the low SG inertia, demonstrating the effectiveness of the modified (weighted mean SM rotor speeds) freezing approach for the mixed GF/SM system. In comparison with Case 12, Fig. 10(a)-(d) show that Case 13 offers a faster active power and voltage recovery for both the GF and SG. The GF has much less overcurrent capability, but by using the proposed GF freezing technique, transient stability is improved for higher GF shares, due to the convenient ability to control the GF angular speed.

Table 4. Simulation settings for Cases 12 and 13

	Proposed freezing control	S_b (MVA) (GF/SG)	H_{SG} (s) (SG)
Case 12	**Yes**	500/500	**0.5**
Case 13	**Yes**	**900/100**	**0.5**

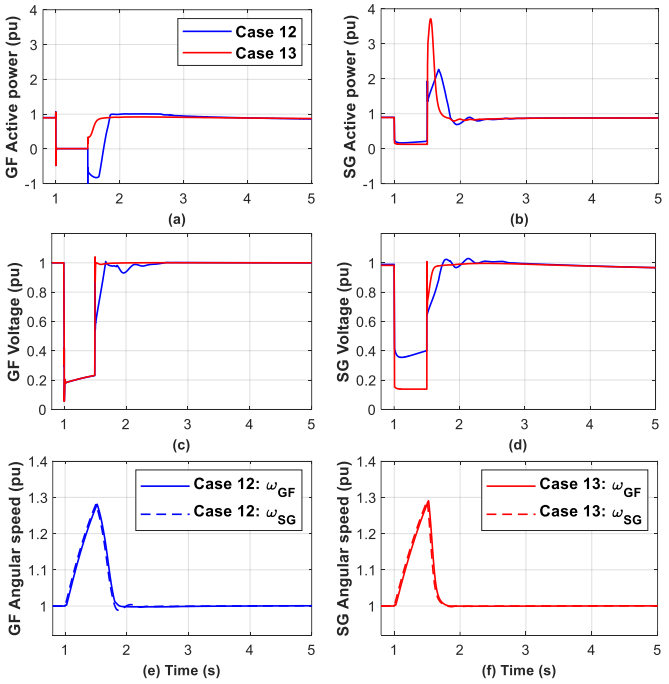

Figure 10. Cases 12 and 13, for mixed GF/SM system, with the modified GF freezing (weighted mean SM rotor speed) technique.

3.5 GF dynamics under phase-jump disturbances

The system of Fig. 1, with the grid represented by an infinite bus in series with a 0.004 pu resistor and 0.02 pu inductor is simulated. Phase jumps of ±60° are applied at the infinite bus, with, and without, incorporating the proposed freezing technique (Fig. 2). Fig. 11 indicates that for both positive and negative phase jumps, the results are unaffected by the presence of the angular speed freezing control. For a phase

jump up event, the GF voltage is high, such that y_v in Fig. 2 remains true, while for a down event, the GF active power is above the pre-fault value, and y_p remains true. Consequently, in neither case does the speed freezing action activate. Note that the proposed control of Fig. 3 is not simulated, as y_v and y_p signals are also used to activate freezing, as Fig. 2.

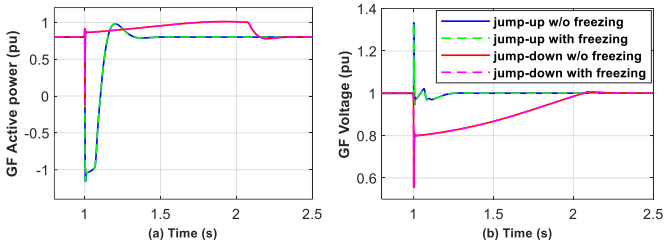

Figure 11. GF response to phase jump (up/down) disturbances.

4. CONCLUSIONS

Strategies to enhance the transient stability of grid-forming converters have tended to focus on systems with a GF connected to an infinite bus, or on 100% GF grids composed of converters with identical control parameters. Recognizing that divergent angular speeds lead to system stability under short-circuit faults, a unified angular speed concept was proposed for GF/SM voltage sources. Specifically, for a 100% GF scenario the virtual angular speeds are frozen to the pre-fault value, while for a mixed GF/SM system, the GF angular speeds are frozen to the weighted mean of the SM rotor speeds. The effectiveness of the approach was shown when applying 500 ms 3-phase faults for different control settings and system conditions, while also being resilient to phase-jump disturbances. Validation on large power system simulations and hardware-in-the-loop experiments will form part of future work.

ACKNOWLEDGEMENTS

Xianxian Zhao is supported by Science Foundation Ireland under Investigator Award SFI/15/IA/3058.

REFERENCES

Cheng, H., Shuai, Z., Shen, C., Liu, X., Li, Z. & Shen, Z. 2020. Transient angle stability of paralleled synchronous and virtual synchronous generators in islanded microgrids. *IEEE Transactions on Power Electronics,* 35, 8751-8765.

Choopani, M., Hosseinian, S. & Vahidi, B. 2019. New transient stability and LVRT improvement of multi-VSG grids using the frequency of the center of inertia. *IEEE Transactions on Power Systems,* 35, 527-538.

Denis, G., Prevost, T., Debry, M., Xavier, F., Guillaud, X. & Menze, A. 2018. MIGRATE project: challenges of operating a transmission grid with only inverter - based generation. A grid-forming control improvement with transient current - limiting control. *IET Renewable Power Generation,* 12, 523-529.

Eskandari, M. & Savkin, A. V. 2020. On the impact of fault ride-through on transient stability of autonomous microgrids: nonlinear analysis and solution. *IEEE Transactions on Smart Grid,* 12, 999-1010.

Hodge, B., Jain, H., Brancucci, C., Seo, G., Korpas, M., Kiviluoma, J., Holttinen, H., Smith, J., Orths, A. & Estanqueiro, A. 2020. Addressing technical challenges in 100% variable inverter - based renewable energy power systems. *Wiley Interdiscipl. Reviews: Energy and Environment,* 9, e376.

Huang, L., Xin, H., Wang, Z., Zhang, L., Wu, K. & Hu, J. 2017. Transient stability analysis and control design of droop-controlled voltage source converters considering current limitation. *IEEE Transactions on Smart Grid,* 10, 578-591.

Kundur, P. 1994. *Power system stability and control*, New York: McGraw-Hill.

Lin, Y., Johnson, B., Gevorgian, V., Purba, V. & Dhople, S. Stability assessment of a system comprising a single machine and inverter with scalable ratings. North American Power Symposium, 2017.

Pan, D., Wang, X., Liu, F. & Shi, R. 2019. Transient stability of voltage-source converters with grid-forming control: A design-oriented study. *IEEE Journal of Emerging and Selected Topics in Power Electronics,* 8, 1019-1033.

Qoria, T., Cossart, Q., Li, C., Guillaud, X., Colas, F., Gruson, F. & Kestelyn, X. 2018. Deliverable 3.2: Local control and simulation tools for large transmission systems. *MIGRATE project*.

Qoria, T., Gruson, F., Colas, F., Denis, G., Prevost, T. & Guillaud, X. 2019. Critical clearing time determination and enhancement of grid-forming converters embedding virtual impedance as current limitation algorithm. *IEEE Journal of Emerging and Selected Topics in Power Electronics,* 8, 1050-1061.

Qoria, T., Rokrok, E., Bruyere, A., Francois, B. & Guillaud, X. 2020. A PLL-free grid-forming control with decoupled functionalities for high-power transmission system applications. *IEEE Access,* 8, 197363-197378.

Rokrok, E., Qoria, T., Bruyere, A., Francois, B. & Guillaud, X. 2021. Transient stability assessment and enhancement of grid-forming converters embedding current reference saturation as current limiting strategy. *IEEE Transactions on Power Systems*.

Shuai, Z., Shen, C., Liu, X., Li, Z. & Shen, Z. J. 2018. Transient angle stability of virtual synchronous generators using Lyapunov's direct method. *IEEE Transactions on Smart Grid,* 10, 4648-4661.

Xiong, X., Wu, C., Cheng, P. & Blaabjerg, F. 2021. An optimal damping design of virtual synchronous generators for transient stability enhancement. *IEEE Transactions on Power Electronics*.

Zhao, F., Wang, X., Zhou, Z., Harnefors, L., Svensson, J. R. & Gryning, M. 2021a. Control interaction modeling and analysis of grid-forming battery energy storage system for offshore wind power plant. *IEEE Transactions on Power Systems*.

Zhao, X. & Flynn, D. Freezing grid-forming converter virtual angular speed to enhance transient stability under current reference limiting. IEEE 21st Workshop on Control and Modeling for Power Electronics, 2020.

Zhao, X., Thakurta, P. & Flynn, D. 2021b. Grid - forming requirements based on stability assessment for 100% converter - based Irish power system. *IET Renewable Power Generation*.